

Contribution from the Laboratory of Chemistry, Nippon Medical School, Kosugi, Nakahara-ku, Kawasaki 211, Japan, and Department of Chemistry, College of Science, Rikkyo University, Nishi-Ikebukuro, Toshima-ku, Tokyo 171, Japan

## Relative Proton Affinity of Neutral Ruthenium(II) Complexes, $[\text{RuX}_2(\text{bpy})_2]$ ( $\text{X} = \text{Cl}, \text{Br}, \text{I}, \text{NCS}, \text{CN}, \text{NO}_2$ ), Observed in Liquid Secondary-Ion Mass Spectrometry Spectra<sup>1</sup>

Mikio Tanaka,\*<sup>†</sup> Takashi Nagai,<sup>†</sup> and Eiichi Miki<sup>†</sup>

Received July 13, 1988

Liquid SIMS spectra for  $[\text{RuX}_2(\text{bpy})_2]$  ( $\text{X} = \text{Cl}, \text{Br}, \text{I}, \text{NCS}, \text{CN}, \text{NO}_2$ ), which are labile to aquation and have poor solubility, were measured. The overlap of isotopic peaks corresponding to the molecular ions of the complexes that have complicated isotopic patterns observed in SIMS spectra could be separated into two components,  $\text{M}^+$  (molecular ion) and  $(\text{M} + \text{H})^+$  (quasi-molecular ion), by pattern analysis. The ratio  $(\text{M} + \text{H})^+/\text{M}^+$  increased in the order  $\text{Cl} < \text{Br} < \text{I} < \text{NCS} < \text{CN} < \text{NO}_2$ , which showed that the differences in the  $\pi$ -acceptor properties of the ligands reflect those of the proton affinities of the ligands. This result was correlated with electrochemical properties and bands in the electronic spectra assigned to  $t_2 \rightarrow \pi^*(1)$  and  $t_2 \rightarrow \pi^*(2)$  for the complexes.

Proton affinities in the gas phase for simple compounds have been measured.<sup>2,3</sup> From ab initio calculations, structures of the protonated molecules have been discussed.<sup>4</sup> Recently, relative proton affinities of four common basic L- $\alpha$ -amino acids were measured from an analysis of metastable cluster ions resulting from FAB MS.<sup>5</sup> However, because complicated metal complexes are difficult to gasify and generally decompose easily when gasification is attempted, the relative proton affinities of the complexes were measured in solution.

Schilt observed that the absorption spectra for  $[\text{Ru}(\text{CN})_2(\text{bpy})_2]$  in glacial acetic acid significantly changed with an increasing concentration of added perchloric acid.<sup>6</sup> He explained that the change arose from the formation of the protonated compounds and discussed the most likely site of protonation. Peterson and Demas reported that  $(\text{D} + \text{H})^+$  and  $(\text{D} + 2\text{H})^{2+}$  ( $\text{D} = [\text{Ru}(\text{CN})_2(\text{bpy})_2]$ ) were present as the protonated species from the relation between  $[\text{H}^+]$  and the solution composition.<sup>7</sup> A difference in the cyanide stretch frequencies between  $[\text{Ru}(\text{CN})_2(\text{bpy})_2] \cdot 3\text{H}_2\text{O}$  recrystallized from water and  $[\text{Ru}(\text{CN})_2(\text{bpy})_2]$  recrystallized from chloroform suggested an interaction between the water of crystallization and the cyanide ligands.<sup>8</sup>

Neutral bis(2,2'-bipyridine)ruthenium(II) complexes,  $[\text{RuX}_2(\text{bpy})_2]$  ( $\text{X} = \text{anionic monodentate ligand}$ ), in particular the dihalogeno complexes, are labile to aquation and have poor solubility in general. Consequently, variations in the proton affinity of neutral metal complexes arising from a systematic change of ligands are difficult to measure. It has been reported that the distribution of ions measured by liquid SIMS reflects the composition of species in the matrix.<sup>9</sup> We have recorded LSIMS spectra for  $[\text{RuX}_2(\text{bpy})_2]$  ( $\text{X} = \text{Cl}, \text{Br}, \text{I}, \text{NCS}, \text{CN}, \text{NO}_2$ ) in glycerol containing 3-mercapto-1,2-propanediol. The overlap of isotopic peaks for the molecular ions of these complexes that have complicated isotopic patterns as observed in the SIMS spectra could be separated into two components,  $\text{M}^+$  (molecular ion) and  $(\text{M} + \text{H})^+$  (quasi-molecular ion), by means of pattern analysis. We have found that the ratio  $(\text{M} + \text{H})^+/\text{M}^+$  increases in the order  $\text{Cl} < \text{Br} < \text{I} < \text{NCS} < \text{CN} < \text{NO}_2$ , and we shall discuss the correlation of this result with the basicity of the ligands, the electrochemical properties, and the bands in electronic spectra assigned to  $t_2 \rightarrow \pi^*(1)$  and  $t_2 \rightarrow \pi^*(2)$ <sup>10</sup> for these complexes. The differences in the  $\pi$ -acceptor properties of the ligands seem to reflect those of the relative proton affinities of the ligands.

### Experimental Section

$[\text{RuCl}_2(\text{bpy})_2] \cdot 3\text{H}_2\text{O}$  was prepared by following the procedure of Tanaka et al.<sup>11</sup>  $[\text{RuBr}_2(\text{bpy})_2]$ ,<sup>12</sup>  $[\text{RuI}_2(\text{bpy})_2]$ ,<sup>12</sup>  $[\text{Ru}(\text{NCS})_2(\text{bpy})_2] \cdot 0.5\text{H}_2\text{O}$ ,<sup>10</sup> and  $[\text{Ru}(\text{CN})_2(\text{bpy})_2]$ <sup>10</sup> were prepared by the literature procedures except that the starting material was  $[\text{Ru}(\text{CO})_3(\text{bpy})_2] \cdot 3\text{H}_2\text{O}$ .<sup>11</sup> The infrared spectrum of the prepared  $[\text{Ru}(\text{NCS})_2(\text{bpy})_2]$  suggested that the NCS ligands are N-bonded.<sup>13</sup>  $[\text{Ru}(\text{NO}_2)_2(\text{bpy})_2]$  was prepared in an analogous manner except that the starting material was  $[\text{Ru}(\text{CO})_3$ -

$(\text{bpy})_2] \cdot 3\text{H}_2\text{O}$ .<sup>11</sup> However, the infrared spectrum showed that the prepared compound contained nitro and nitrito ligands. This mixed complex was refluxed in methanol under nitrogen for 16 h, and complete conversion to the dinitro complex was confirmed by infrared spectroscopy.<sup>14</sup> The values of elemental analyses for the complexes agreed with the calculated values within experimental error margins. The electronic spectra in  $\text{CH}_2\text{Cl}_2$  were measured with a Hitachi 330 spectrophotometer.

**Instrumentation. Liquid SIMS.** A Hitachi M-80 double-focusing mass spectrometer equipped with a Hitachi M-003 data-processing system was used. The liquid SIMS spectra were recorded by the mass spectrometer with a positive SIMS unit. The complexes were suspended and/or dissolved in 3-mercapto-1,2-propanediol containing  $15.6 \pm 0.8$  wt % of glycerol and were placed on a silver probe tip. Xenon was used to produce the primary ion. The primary-ion accelerating potential was 8 kV.

**Pattern Analysis.** We thought that the isotopic clusters corresponding to molecular ions consisted of an overlap of isotopic peaks for two chemical species,  $(\text{M} + \text{H})^+$  and  $\text{M}^+$ , as will be discussed later. The relative intensities of the isotopic peaks of  $(\text{M} + \text{H})^+$  and  $\text{M}^+$  were calculated in consideration of the isotopic abundances of all of the constituent elements contained in the complexes. The combinational ratio of the chemical species,  $(\text{M} + \text{H})^+$  and  $\text{M}^+$ , was calculated by a least-squares method to minimize the difference in the intensity between the observed and calculated isotopic clusters. Isotopic peaks with relative intensities larger than 0.1% were used for the calculation.

### Results and Discussion

Because the ruthenium atom has seven stable isotopes and the majority of the other constituent elements have some stable isotopes, the range of  $m/z$  for the molecular ions is more than 10. For example, there are 15 mass spectral peaks calculated for the molecular ion of  $[\text{RuCl}_2(\text{bpy})_2]$  having relative intensities larger than 0.1%. The range of  $m/z$  for the molecular ions observed in liquid SIMS spectra was more than 10, and isotopic clusters for the molecular ions were observed as complicated isotopic patterns in the spectra, as shown in Figure 1. Chemical species contained in isotopic peaks observed on the SIMS spectrum were

- (1) SIMS and FD Mass Spectrometry of Metal Complexes. 2. Part 1: Tanaka M.; Miki, E. *Chem. Lett.* **1985**, 1755.
- (2) Moeller, T. *Inorganic Chemistry: A Modern Introduction*; Wiley-Interscience: New York, 1982; Chapters 4 and 9. Huheey, J. E. *Inorganic Chemistry: Principles of Structure and Reactivity*, 3rd ed.; Harper and Row: New York, 1983; Chapter 7.
- (3) Baer, T. In *Mass Spectrometry*; Johnstone, R. A. W., Senior Reporter; Specialist Periodical Report; The Chemical Society: London, 1981; Vol. 6, Chapter 1.
- (4) Karpas, Z.; Stevens, W. J.; Buckley, T. J.; Metz, R. *J. Phys. Chem.* **1985**, *89*, 5274.
- (5) Bojesen, G. *J. Chem. Soc., Chem. Commun.* **1986**, 244.
- (6) Schilt, A. A. *J. Am. Chem. Soc.* **1963**, *85*, 904.
- (7) Peterson, S. H.; Demas, J. N. *J. Am. Chem. Soc.* **1976**, *98*, 7880.
- (8) Schilt, A. A. *Inorg. Chem.* **1964**, *3*, 1323.
- (9) De Pauw, E. *Mass Spectrom. Rev.* **1986**, *5*, 191.
- (10) Bryant, G. M.; Fergusson, J. E.; Powell, H. K. *J. Aust. J. Chem.* **1971**, *24*, 257.
- (11) Tanaka, M.; Nagai, T.; Miki, E.; Mizumachi, K.; Ishimori, T. *Nippon Kagaku Kaishi* **1979**, 1112.
- (12) Fergusson, J. E.; Harris, G. M. *J. Chem. Soc. A*, **1966**, 1293.
- (13) Durham, B.; Walsh, J. L.; Carter, C. L.; Meyer, T. *J. Inorg. Chem.* **1980**, *19*, 860.
- (14) Adeyemi, S. A.; Miller, F. J.; Meyer, T. *J. Inorg. Chem.* **1972**, *11*, 944.

<sup>†</sup> Nippon Medical School.

<sup>†</sup> Rikkyo University.

**Table I.** Percentages of  $(M + H)^+$  and  $M^+$ , Absorption Spectral Data, and Electrochemical Properties of  $[\text{RuX}_2(\text{bpy})_2]$ 

complexes	percentage		band energy/cm <sup>-1</sup>		$E_{1/2}(\text{Ru}^{\text{III/II}})/\text{V}$
	$(M + H)^+$	$M^+$	$t_2 \rightarrow \Pi^*(1)$	$t_2 \rightarrow \Pi^*(2)$	
$[\text{RuCl}_2(\text{bpy})_2]^a$	$9 \pm 1^g$	$92 \pm 1$	17 900	26 300	$0.31^h$ (in $\text{CH}_3\text{CN}$ )
$[\text{RuBr}_2(\text{bpy})_2]^b$	$17 \pm 2$	$83 \pm 2$	18 100	26 500	$0.37^h$ (in $\text{CH}_3\text{CN}$ )
$[\text{RuI}_2(\text{bpy})_2]^c$	$34 \pm 4$	$66 \pm 4$	18 200	26 800	
$[\text{Ru}(\text{NCS})_2(\text{bpy})_2]^d$	$48 \pm 5$	$52 \pm 5$	19 200	27 500	$0.67^h$ (in $\text{CH}_3\text{CN}$ )
$[\text{Ru}(\text{CN})_2(\text{bpy})_2]^e$	$87 \pm 2$	$13 \pm 2$	20 000	28 800	$0.85^i$ (in DMF)
$[\text{Ru}(\text{NO}_2)_2(\text{bpy})_2]^f$	$90 \pm 2$	$10 \pm 2$	21 200	29 700	

<sup>a-f</sup> Number of runs; concentration range/mmol matrix g<sup>-1</sup>; standard deviation: (a) 6;  $5.0 \times 10^{-2}$ – $1.5 \times 10^{-1}$ ; 0.033. (b) 20;  $3.3 \times 10^{-3}$ – $1.1 \times 10^{-1}$ ; 0.046. (c) 12;  $3.5 \times 10^{-3}$ – $2.9 \times 10^{-2}$ ; 0.055. (d) 11;  $2.8 \times 10^{-3}$ – $4.2 \times 10^{-2}$ ; 0.048. (e) 15;  $3.2 \times 10^{-3}$ – $8.7 \times 10^{-2}$ ; 0.033. (f) 10;  $4.6 \times 10^{-3}$ – $9.6 \times 10^{-2}$ ; 0.036. <sup>g</sup> 1 $\sigma$  standard deviation. <sup>h</sup> See ref 13. <sup>i</sup> See ref 18.

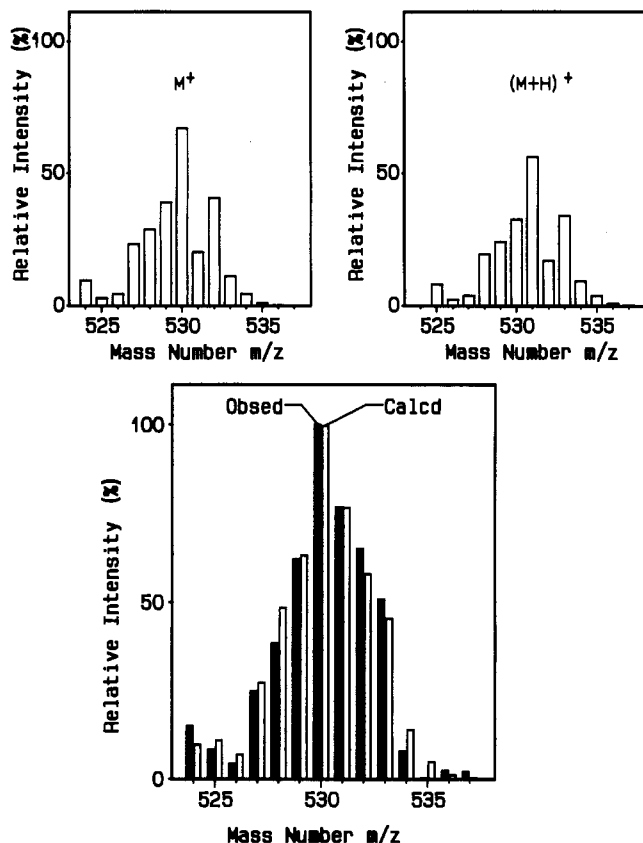


**Figure 1.** Pattern analysis for the overlap of isotopic clusters corresponding to molecular ions of  $[\text{Ru}(\text{NCS})_2(\text{bpy})_2]$  observed in the liquid SIMS spectrum (standard deviation = 0.048).

identified by  $m/z$  of the peak with the largest intensity in the peaks corresponding to  $m/z$  of the molecular ions. Major chemical species in the peaks were  $M^+$  for  $[\text{RuCl}_2(\text{bpy})_2]$  and  $(M + H)^+$  for  $[\text{Ru}(\text{NO}_2)_2(\text{bpy})_2]$ . This result shows that isotopic clusters corresponding to the molecular ion consist mainly of the overlap of isotopic peaks for two chemical species,  $M^+$  and  $(M + H)^+$ . From this conception, the combinational ratio of two chemical species for the molecular ion was calculated by pattern analysis. The difference in the intensity between the observed and the calculated isotopic peaks was small, as shown in Table I.

The analyzed example for  $[\text{Ru}(\text{NCS})_2(\text{bpy})_2]$  is shown in Figure 1. Percentages of  $M^+$  and  $(M + H)^+$  in the isotopic clusters corresponding to the molecular ions for  $[\text{RuX}_2(\text{bpy})_2]$  are shown in Table I. The ratio  $(M + H)^+/M^+$  increased in the order  $\text{Cl} < \text{Br} < \text{I} < \text{NCS} < \text{CN} < \text{NO}_2$ .

After  $[\text{RuCl}_2(\text{bpy})_2]$  dissolved in dichloromethane had been placed on a carbon emitter, the FD mass spectrum was recorded. A pattern analysis for isotopic clusters corresponding to the molecular ion observed in the FD mass spectrum indicated that the difference in intensity between the observed and the calculated isotopic clusters was minimum (standard deviation = 0.012) when  $M^+$  and  $(M + H)^+$  were 100% and 0%, respectively.<sup>1</sup> On the other hand, pattern analysis for the SIMS spectrum of the dichloro

complex indicated that  $M^+$  and  $(M + H)^+$  were 91% and 9%, respectively. The differences in combinational ratio between the isotopic clusters observed in the FD mass spectrum and the SIMS spectrum indicates that protons derived from the matrix are mainly attributable to the addition of protons to the complexes.

The optimum condition for measurement of the SIMS spectra was the use of glycerol (15.6  $\pm$  0.8 wt. %) in 3-mercapto-1,2-propanediol. The concentration range of the complexes in the matrix is also shown in Table I. No change in the ratio  $(M + H)^+/M^+$  was observed in the concentration range. Nor did this ratio change when the concentration of glycerol in 3-mercapto-1,2-propanediol was varied. From these results, the differences in the ratios  $(M + H)^+/M^+$  caused by the change of X in  $[\text{RuX}_2(\text{bpy})_2]$  appears to arise from the inherent characteristics of the complexes.

Fluorometric measurements of  $[\text{Ru}(\text{CN})_2(\text{bpy})_2]$  (D) in aqueous solution showed that the predominant species changed from D to  $(D + H)^+$  and  $(D + 2H)^{2+}$  successively with an increasing concentration of perchloric acid.<sup>7</sup> However, isotopic clusters corresponding to  $(M + 2H)^{2+}$  ( $M = [\text{Ru}(\text{CN})_2(\text{bpy})_2]$ ) could not be found in the SIMS spectrum.

A  $pK_b$  of HX increases in the order  $\text{HI} < \text{HBr} < \text{HCl} < \text{HNCS} < \text{HNO}_2 < \text{HCN}$ .<sup>15</sup> This order of  $pK_b$  was not consistent with that of the ratio  $(M + H)^+/M^+$ .

The examined complexes have two intense bands around 20 000 and 27 000  $\text{cm}^{-1}$ , as shown in Table I. The bands have been assigned to ruthenium-to-bipyridine charge transfer,  $t_2(\text{Ru}) \rightarrow \pi^*(\text{bpy})$ .<sup>10</sup> The position of maximum absorption shifted to higher energy in the order  $\text{Cl} < \text{Br} < \text{I} < \text{NCS} < \text{CN} < \text{NO}_2$  in dichloromethane. Strongly solvatochromic shifts were observed for  $[\text{Ru}(\text{CN})_2(\text{bpy})_2]$  and  $[\text{Ru}(\text{NO}_2)_2(\text{bpy})_2]$  in methanol or dimethyl sulfoxide. But there seems to be no shift in dichloromethane because the interaction of the complex with dichloromethane is generally weak.<sup>16</sup> Thus, the position of the band in dichloromethane appears to reflect the inherent properties of these complexes. As X in the examined complexes changes in the above order, the  $t_2$  electrons in the ruthenium are better stabilized by the electron-withdrawing ligand, X. This causes an increase in the energy of the transition  $t_2 \rightarrow \pi^*$ . The band shifts have been explained by the  $\pi$ -acceptor properties of the ligands.<sup>17</sup> The  $\pi$ -acceptor properties of the ligands would increase in the above order for  $[\text{Ru}^{\text{II}}\text{X}_2(\text{bpy})_2]$ .

The contribution of  $\sigma$  components could not be discussed because the assignment of the absorption band involved in the e level is ambiguous for the complexes examined.

Electrochemical data for  $[\text{RuX}_2(\text{bpy})_2]$  (X = Cl, Br, NCS, CN) are shown in Table I. The order of  $E_{1/2}(\text{Ru}^{\text{III/II}})$  for these complexes was  $\text{Cl} < \text{Br} < \text{NCS} < \text{CN}$ .<sup>13,18</sup> The  $\pi$ -acceptor ligand

- (15) *Stability Constants of Metal-Ion Complexes*; Hogfeldt, E., Ed.; Pergamon: New York, 1982; Part A. *Stability Constants of Metal-Ion Complexes*; Sillen, L. G., Martell, A. E., Eds.; Special Publication No. 17; The Chemical Society: London, 1964. *Stability Constants of Metal-Ion Complexes, Supplement No. 1*; Sillen, L. G., Martell, A. E., Eds.; Special Publication No. 25; The Chemical Society: London, 1971.
- (16) Gutmann, V. *The Donor-Acceptor Approach to Molecular Interactions*; Plenum: New York, 1978; Chapter 2.
- (17) Johnson, C. R.; Shepherd, R. E. *Inorg. Chem.* **1983**, *22*, 2439.
- (18) Roffia, S.; Ciano, M. J. *Electroanal. Chem. Interfacial Electrochem.* **1977**, *77*, 349.

withdraws the ruthenium center's intrinsic valence-shell electron, and the reduction potentials are largely due to the  $\pi$ -acceptor ability of the ligands in ruthenium(II) complexes.<sup>19,20</sup> Thus, the electrochemical properties show that  $\pi$ -acceptor ability increases in the order  $\text{Cl} < \text{Br} < \text{NCS} < \text{CN}$ .

The tendency observed in the SIMS spectra of proton affinity to increase in the examined complexes was consistent with that of the  $t_2 \rightarrow \pi^*$  transition energy and  $E_{1/2}$ .

From measurement of the electronic spectrum for  $[\text{Ru}(\text{CN})_2(\text{bpy})_2]$  in strongly acidic solution, Schilt reported that the nitrogen atom of the cyanide group was the most likely site for

protonation.<sup>6</sup> We thought that a proton would bind to the anionic ligands because the electronegativity of the ligands increases to the extent that the  $\pi$ -acceptor property of the ligands increases in the complexes.

For low-volatility and thermally unstable complexes such as  $[\text{RuX}_2(\text{bpy})_2]$  in which the ruthenium atom has seven stable isotopes with comparatively large abundances, a difference in proton affinity between the complexes arising from replacement of monodentate anionic ligands was found from measurement of liquid SIMS spectra. Pattern analysis is a useful and powerful method for correlating the results obtained from liquid SIMS spectra with characteristics of the complexes obtained by other methods.

**Acknowledgment.** We wish to express our sincere thanks to Dr. Shinzaburo Hishida (Hitachi, Ltd.) for his helpful suggestions.

- (19) Connor, J. A.; Meyer, T. J.; Sullivan, B. P. *Inorg. Chem.* **1979**, *18*, 1388.  
 (20) Johnson, C. R.; Shepherd, R. E. *Synth. React. Inorg. Met.-Org. Chem.* **1984**, *14*, 339.

Contribution from the Department of Chemistry,  
 Texas A&M University, College Station, Texas 77843

## X-ray Powder Structure and Rietveld Refinement of the Monosodium-Exchanged Monohydrate of $\alpha$ -Zirconium Phosphate, $\text{Zr}(\text{NaPO}_4)(\text{HPO}_4)\cdot\text{H}_2\text{O}$

Philip R. Rudolf and Abraham Clearfield\*

Received August 8, 1988

The crystal structure of the partially hydrated monosodium-exchanged phase of  $\alpha$ -zirconium phosphate,  $\text{Zr}(\text{HPO}_4)_2\cdot\text{H}_2\text{O}$ , has been determined by using data collected on a conventional computer-controlled X-ray powder diffractometer. The positions of all atoms in the layer were determined by using 40 unambiguously indexed reflections, obtained by pattern decomposition, in a conventional single-crystal type analysis. Whole-pattern (Rietveld) analysis was then conducted to  $R_{\text{wp}} = 0.156$  and resulted in the location and refinement of the exchanged  $\text{Na}^+$  ion and the water oxygen in the interlamellar space.  $\text{Zr}(\text{NaPO}_4)(\text{HPO}_4)\cdot\text{H}_2\text{O}$  is monoclinic,  $P2_1/c$ , with cell parameters  $a = 8.8264$  (2) Å,  $b = 5.3494$  (1) Å,  $c = 16.0275$  (6) Å,  $\beta = 101.857$  (4)°, and  $Z = 4$ . The structure is a modification of the parent  $\alpha$ -zirconium phosphate with a shift of adjacent layers and twisting of the phosphate groups. This results in an altered cavity arrangement.  $\text{Na}^+$  lies in a distorted octahedral environment, as does the water oxygen, O12. This arrangement of atoms in the interlamellar region is in an ordered manner similar to that in  $\text{Zr}(\text{NH}_4\text{PO}_4)_2\cdot\text{H}_2\text{O}$ . Loss of the 1 mol of water results in a change in space group, and a mechanism for this transformation as well as that of the exchange process will be described.

### Introduction

Zirconium bis(monohydrogen orthophosphate) monohydrate,  $\text{Zr}(\text{HPO}_4)_2\cdot\text{H}_2\text{O}$  or  $\alpha$ -ZrP, is a microcrystalline powder with a layered structure.<sup>1</sup> The phosphate hydrogens may be exchanged for mono- and divalent cations, resulting in a large number of half-exchanged and fully exchanged phases.<sup>2</sup> For each exchange ion there exists a number of phases that represent different hydrates as well as anhydrous phases.<sup>2,3</sup>

In the parent  $\alpha$ -ZrP<sup>1,4</sup> the Zr atoms lie nearly in a plane and are bridged by the phosphate groups, which alternate above and below the level of the plane. Three oxygens of each phosphate group are bonded to three different zirconium atoms arranged at the apices of a near-equilateral triangle. The fourth oxygen points away from the layer and into the interlamellar region. These oxygens, labeled O7 and O10, are bonded to protons. Adjacent layers are staggered, resulting in hexagonal-capped cavities between the layers. A water molecule resides in the center of each cavity. The adjacent layers are held together solely by van der Waals forces, and they are able to expand or contract as a result of ion exchange or intercalation processes. The ion-exchanged zirconium phosphates are readily identified by their characteristic basal  $d$ -spacing in the X-ray powder pattern, and relationships between basal  $d$ -spacing and the amount of water of crystallization in the structure are well-known.<sup>5</sup>

Single crystals of  $\alpha$ -ZrP may be prepared by a variety of methods.<sup>1,6</sup> However, ion exchange on such crystals results in loss of some crystallinity as the layers disorder.<sup>7</sup> Retention of

the crystalline structure on ion exchange is accomplished by exchanging microcrystalline  $\alpha$ -ZrP in buffered solutions by slow potentiometric titration.<sup>8,9</sup> The product is a microcrystalline powder. However, even when good-quality single crystals are used for exchange, the product is so disordered that it cannot be used for structure solutions by standard single-crystal methods. Thus, the single-crystal structure of only one exchanged phase,  $\text{Zr}(\text{NH}_4\text{PO}_4)_2\cdot\text{H}_2\text{O}$ , has been obtained previously.<sup>10</sup> This structure solution was possible because ammonia is taken up by intercalation rather than ion exchange and forms ammonium ions at the proton sites.<sup>11</sup> Apparently, the intercalation process with a small molecule does not greatly disorder the layers as the resultant phase was found to have a structure very similar to that of the parent acid.

Given the problem with the exchanged phases, we undertook to solve their structures by powder methods.<sup>12,13</sup> To make the

- (1) Clearfield, A.; Smith, G. D. *Inorg. Chem.* **1969**, *8*, 431.  
 (2) Clearfield, A. *Zirconium Phosphates*. In *Inorganic Ion Exchange Materials*; Clearfield, A., Ed.; CRC Press: Boca Raton, FL, 1982; p 16.  
 (3) Clearfield, A.; Duax, W. L.; Medina, A. S.; Smith, G. D.; Thomas, J. R. *J. Phys. Chem.* **1969**, *73*, 3424.  
 (4) Troup, J. M.; Clearfield, A. *Inorg. Chem.* **1977**, *16*, 3311.  
 (5) Alberti, G. *Acc. Chem. Res.* **1978**, *11*, 163.  
 (6) Alberti, G.; Torracca, E. *J. Inorg. Nucl. Chem.* **1968**, *30*, 317.  
 (7) Alberti, G.; Costantino, U.; Giulietti, R. *J. Inorg. Nucl. Chem.* **1980**, *42*, 1062.  
 (8) Clearfield, A.; Medina, A. S. *J. Inorg. Nucl. Chem.* **1970**, *32*, 2775.  
 (9) Clearfield, A.; Duax, W. L.; Garcés, J. M.; Medina, A. S. *J. Inorg. Nucl. Chem.* **1972**, *34*, 329.  
 (10) Clearfield, A.; Troup, J. M. *J. Phys. Chem.* **1973**, *77*, 243.  
 (11) Alberti, G.; Bertrami, R.; Costantino, U.; Gupta, J. P. *J. Inorg. Nucl. Chem.* **1977**, *39*, 1057.  
 (12) Rudolf, P. R. Ph.D. Dissertation, Texas A&M University, May 1983.

\* To whom correspondence should be addressed.